Original Manuscript

New hybrid approach HNSGA-III&SPEA/R: Application to optimization of powertrain mount system stiffness parameters

Nguyễn H Trưởng[1] and Dinh-Nam Dao[2,3] (iD)

Abstract

In this study, a new methodology, hybrid NSGA-III with SPEA/R (HNSGA-III&SPEA/R), has been developed to design and achieve cost optimization of powertrain mount system stiffness parameters. This problem is formalized as a multi-objective optimization problem involving six optimization objectives: mean square acceleration and mean square displacement of the powertrain mount system. A hybrid HNSGA-III&SPEA/R is proposed with the integration of Strength Pareto evolutionary algorithm based on reference direction for Multi-objective (SPEA/R) and Many-objective optimization genetic algorithm (NSGA-III). Several benchmark functions are tested, and results reveal that the HNSGA-III&SPEA/R is more efficient than the typical SPEA/R, NSGA-III. Powertrain mount system stiffness parameters optimization with HNSGA-III&SPEA/R is simulated respectively. It proved the potential of the HNSGA-III&SPEA/R for powertrain mount system stiffness parameter optimization problem.

Keywords

HNSGA-III&SPEA/R, NSGA-III, SPEA/R, optimal solution, powertrain mount system stiffness

Introduction

The vehicle's power source system, including engines, transmission, and clutches, is the source of energy for vehicles and is also one of the main sources of vibration in the vehicle. Therefore, the engine mount is usually installed between the power source system and the car body to isolate the vibration transmitted from the power source system to the body as Yu and Naganathan.[1] The system consists of mounts, and power source system is powertrain mount system. In a full-car dynamics system, the mounts play an important role, and the principle diagram of a full-car dynamic model with a power source system mounting system is shown in Figure 1. Good powertrain system mounts will improve the performance of vibration and noise and harshness (NVH) of the vehicle while extending the life of the engine and related parts which is pointed out as Adiguna et al.[2] Engine mounts can be categorized according to the characteristics of the ability to control of mounts as passive mounts (rubber mounts and hydraulic mounts are the most popular), active mounts, and semi-active mounts. Typically, rubber mounts include a metal frame where the rubber is bonded through adhesives or during vulcanization. Rubber mounts are the most widely used engine mounts for their low cost and simple structure. In order to design high-quality mounts as required, the parameters of the mounts must match their stiffnesses. Mounts with good

[1]Institute of Military Mechanical Engineering, Cầu Giấy, Ha Noi, Vietnam
[2]School of Mechanical Engineering and Automation, Northeastern University, Shenyang, China
[3]Control Technology College, Le Quy Don Technical University, Hanoi, Vietnam

Corresponding author:
Dinh-Nam Dao, School of Mechanical Engineering and Automation, Northeastern University, No. 3-11, Wenhua Road, Heping District, Shenyang 110819, China.
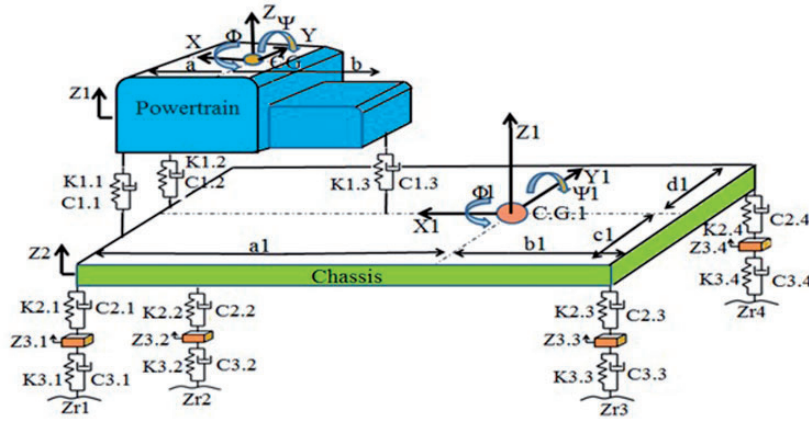Email: daodinhnambkc@gmail.com

Figure 1. The principle diagram of a full-car dynamic model with a power source system mounting system.

stiffnesses not only reduce the vibration of the engine transmitting to the elastic substrate (such as frame and body) but also reduce the undesirable effect of stimuli from the road and the wheel impacting on the body car. Therefore, an important task in designing the power source system mounting system is to calculate the optimal stiffness parameters for the power source system mounting system. This is a multi-object optimization issue. Figure 1 shows the specific model of the motor bearing system.

In recent years, several researchers have been studying in this field, and different methods with different capabilities were developing that many of them were presented in an overview and tutorial.[3] NSGA-II was developed by Deb et al.,[4] and till date, several variants and applications for NSGA II have been developed by Chang and Chang.[35] Ishibuchi et al.[6] and Malekmohammadi et al.,[7] and Kalyanmoy[8] proposed applying MONGA-II to a number of many-objective test problems. NSGA-III is designed to face multiple goals at once (more than two). This algorithm is proposed by Deb and Jain[9] to change some selection mechanisms. Here, they proposed a Multi-objective evolution algorithm based on the reference point according to the NSGA-II framework, emphasizing that the population is not common, but close to a set of reference points provided. The proposed NSGA-III is applied to a number of multi-objective testing issues with 3–15 goals.

In addition, the Pareto 2 strong evolutionary algorithm (SPEA2) is an extended version of SPEA's multi-objective evolution optimization algorithm. This algorithm uses a mechanism such as k-Recent Neighbor (kNN) and a specialized ranking system to align members of the population and choose the next generation of population from the combination of the current population in and out of the stream created by genetic operators (mutations and crossover). SPEA2 is one of the most well-known and most useful multi-objective optimization algorithms and is widely used and applied to handle real-world scientific and technical applications. There are some researchers on this algorithm as well. Kim et al.[10] propose two new mechanisms to be added to SPEA2 to improve its searchability for a more efficient cross-mechanism and storage mechanism to maintain the diversity of solutions in the target space and transform. Zitzler et al.[11] proposed an SPEA2: Improving the Pareto evolution algorithm to power multi-objective optimization. Borisevic and Bartlett[12] proposed a design optimization scheme using multi-objective genetic algorithms applied to offshore platform processes. Optimization criteria relate to unavailability, cost, fake trip, and maintenance downtime to obtain an optimal safety system design. Hiroyuki and Hiroki[13] proposed a new method to assess the probability reliability with multi-target super therapy (MOMH) in the smart grid. It is very useful to evaluate a set of Pareto solutions in a systematic way. Inside, SPEA2 (Intensity 2 Evolutionary Algorithm) is used to evaluate the Pareto solution due to the good performance of a variety of solutions different from normal multi-objective reliability assessment. De Tommasi et al.[14] have proposed a multi-objective optimization for radio-frequency circuit blocks through replacement models and NBI and SPEA2 methods. Sokratis and George[15] proposed a model-based machine translation system using large monolithic blocks in the target language from which statistical information was extracted. This study reported using a specific machine translation to represent the test that SPEA2 was chosen as the optimization method. Zhao et al.[16] proposed an SPEA2 algorithm based on adaptive selection evolutionary operators. The proposed algorithm can selectively adapt simulated binary interference, polynomial mutations, and differential evolutionary operators in their evolution according to their contribution to the external repository. Imen et al.[17] proposed SPEA2 for the

Economic/Environmental Power Distribution problem. In the past, minimizing fuel costs is the only objective function of economic power coordination. Due to the modification of clean air, behavior has been applied to reduce emissions of polluting emissions from power plants, and utilities have also changed strategies to reduce pollution and atmospheric emissions, minimizing generation waste when other target functions turn economic capacity into versatile-objective problem with conflicting goals. Jiang and Yang[18] published a new SPEA based on the reference direction, denoted SPEA/R, to optimize multiple goals. A significant extension of the early SPEA algorithms is SPEA/R. It applies to the advantage of SPEA2's physical assignment in quantifying solutions diversity and convergence in one method. It is appropriate to replace the most time-consuming density estimator with an algorithm based on the reference direction. Their proposed exercise duties also take into account the convergence both local and global.

Recently, there are a number of multi-objective optimization algorithms that have been proposed. Some of these new studies include the Multi-objective gray wolf optimizer[19] and Optimizing multi-target cats.[20] Velazquez et al.[21] proposed Multi-objective differential evolution, Hemmatian[22] proposed Multi-objective gravitational search algorithm, Shi and Kong[23] proposed a Multi-objective ant colony optimization algorithm based on elitist selection strategy, Hancer et al.[24] proposed a multi-objective artificial bee colony approach to feature selection using fuzzy mutual information, and Lin et al.[25] proposed the Multi-objective teaching-learning-based optimization algorithm. Because they cannot solve all optimization problems correctly even though all algorithms can approximate the true Pareto optimal front of a given problem. Therefore, new hybrid algorithms need to be proposed to be able to solve new problems that have not been resolved before and/or to have better accuracy than existing techniques.

Some methods of hybridization of optimal algorithms have been developed recently: Jeong et al.[26] proposed the development and investigation of Efficient GA/PSO-hybrid algorithm applicable to real-world design optimization; Premalatha et al.[20] proposed Hybrid PSO and GA for global maximization; Bai[27] proposed a way to optimize multi-target particles based on extreme optimization with variable and inertial inertia mutations to improve the performance of the algorithm while solving some problems in multi-target particle optimization. A new hybrid heuristic optimization method is published in the current work for multi-purpose issues. A hybrid method is proposed to combine the simple method of Nelder–Mead with the non-dominance sequencing method (NSGA II) to find the best global point. In order to evaluate the performance of the new proposed method, it has been shown through some complex standard functions of Zandavi.[28] Yang et al.[29] proposed a Generate-first-choose-later algorithm to solve multivariate technical optimization problems so that Pareto solutions can be set and optimize multiple times until satisfactory results are obtained. An effective method consists of independent parallel genetic algorithms by dividing the entire population into multiple populations by Rashidi et al.[30] Each population group is assigned to different weights to search for optimal solutions in different directions. Thus, most published hybrid algorithms have more advantages. This hybridization has overcome the limitations of each optimization algorithm. This proves that this is one of the methods that need to be studied in multi-objective optimization.

In this article, a new hybrid optimization method is proposed in the current work for multi-objective problems. This is the hybrid between the Strength Pareto evolutionary algorithm based on reference direction for Multi-objective (SPEA/R) and Many-objective optimization genetic algorithm (NSGA-III) to find the best of the Pareto-optimal front. The performance of the new algorithm is demonstrated via some complex benchmark functions and for powertrain mount system stiffness parameter optimization problem with six-objective optimization in model 3D.

The organization of this paper is as follows: "Structure" section describes the proposed hybrid HNSGA-III&SPEA/R method and computational experimentation with several benchmark functions. "Vibration characteristic of the powertrain mount system" section describes the vibration characteristic of the powertrain mount system and simulation results of application HNSGA-III&SPEA/R method to optimization of the powertrain mount system stiffness parameter. Finally, a conclusion is given.

Structure

Many-objective optimization Genetic Algorithm NSGA-III

Deb and Jain[9] improved the NSGA-II gene algorithm into NSGA-III. The NSGA-III algorithm is based on the steps described in flowchart of NSGA-III as shown in Figure 2.
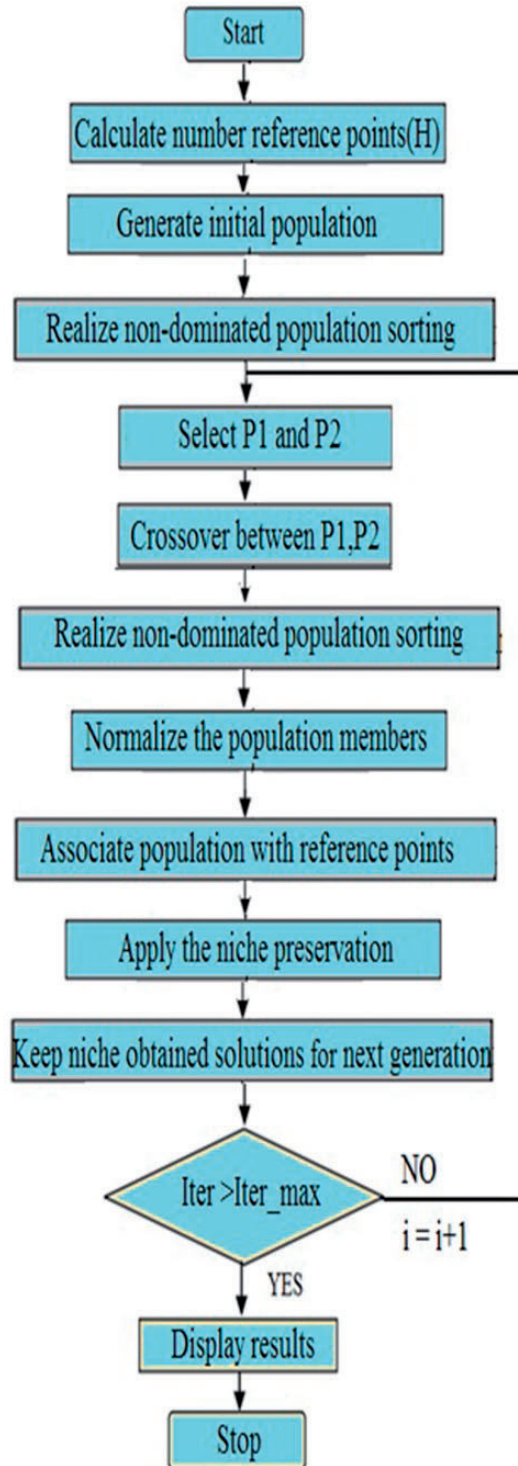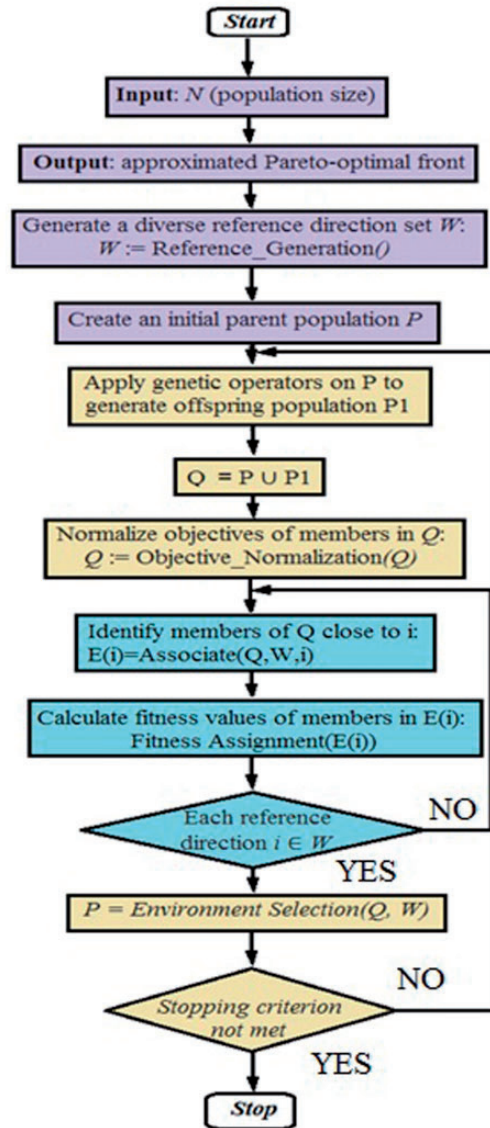
Figure 2. Flowchart of of NSGA-III.

Figure 3. Flowchart of SPEA/R.

SPEA/R algorithm

Jiang and Yang[18] proposed SPEA/R algorithm, and it is presented in the flowchart of SPEA/R as shown in Figure 3.

Hybrid NSGA-III and SPEA/R (HNSGA-III&SPEA/R)

Evolutionary algorithms have different strengths and weaknesses. They can handle complex problems. We often think of integrating different algorithms. In the field of research, they consolidate different methods of evolution or optimization algorithms into a single algorithm. More efficient hybrid algorithms can exchange each other's strengths; all shown in the results indicate that. It can be processed in parallel, can improve exploration and exploitation, and can yield more favorable performance than any single algorithm. These population-based approaches use different techniques to explore the search space, and when they are combined, it will improve the trade-off between exploration and exploitation tasks to converge solutions. The best solution possible. This hybrid has acquired the strengths of both algorithms, which are fast convergence capabilities in NSGA-III and SPEA/R diverse search capabilities, thus reducing the computation time, and Pareto front is more accurate than the above two methods.

HNSGA-III&SPEA/R hybrid approach. HNSGA-III&SPEA/R is implemented in parallel hybridization. That is, the original population will be both NSGA-III and SPEA/R simultaneously generated. After that, two separate populations will be mixed together. The new population after the mix will be both algorithms used as their own population to perform evaluation fitness function calculations for the evolution of each algorithm. To the next generation, the new population that is created by the two algorithms is mixed together to form a common population. The process repeats until the evolutionary termination condition is complete.

The pseudo code of the proposed algorithm. Initialize parameters for NSGA-III and SPEA/R.
  SPEA/R: Swarm population initialization.
  NSGA-III: GA population initialization.
  While travel not completed.
  Mix the two populations.
  Call SPEA/R algorithm.
  While *stopping criterion not met* do
  Use genetic elements on P to produce the female population P
  $Q = P \cup P$
  Normalize the members' goals in Q: $Q = $ Objective_Normalization(Q)
  For each reference direction $i \in W$ do

  Assign members of Q close to i:

  $E(i) = $ Associate(Q, W, i)

  Determine the physical value of members in $E(i)$:Fitness_Assignment$(E(i))$
  End for
  $P = $ Environment_Selection(Q, W)
  End while.
  Call NSGA-III algorithm.
  While evolution not completed.
  Assign two parents $P1$ and $P2$ using the tournament method.
  Assign the crossover between $P1$ and $P2$ with a probability Pc.
  Realize the non-dominated population sorting.
  Normalize the population members.
  Associate the population member with the reference Points.
  Assign the niche preservation (counter).
  Keep the niche obtained solutions for the next generation.
  End while.
  End while.
  A flowchart of HNSGA-III&SPEA/R is shown in Figure 4.

Computational experimentation with several benchmark functions

Numerical results. In this section, the performance of HNSGA-III&SPEA/R is proved by the five standard functions proposed in CEC 2009,[31] listed in Table 1. The results are compared to the methods of NSGA-III and Multi-objective SPEA/R. Inverted generational distance (IGD) of Schott criteria are employed to measure convergence, quantity, and coverage, respectively. The mathematical formulation of IGD is as follows

$$IGD = \frac{\sqrt{\sum_{i=1}^{N} d_i^2}}{N} \tag{1}$$

where N is the number of real Pareto optimal solutions and d_i shows the Euclidean distance between the correct ith Pareto optimal solution and the cabinet to obtain Pareto optimal solutions in the reference set. It should be noted that IGD $= 0$ indicates that all members of non-dominant solutions are in the real Pareto Front.

In addition to using performance data, the best Pareto optimization solution set by HNSGA-III&SPEA/R on both parameter space and search space is shown in Figure 5 (UF1, UF4, and UF5). These figures clearly show the performance of HNSGA-III&SPEA/R compared to the true Pareto front. For comparison and evaluation, these
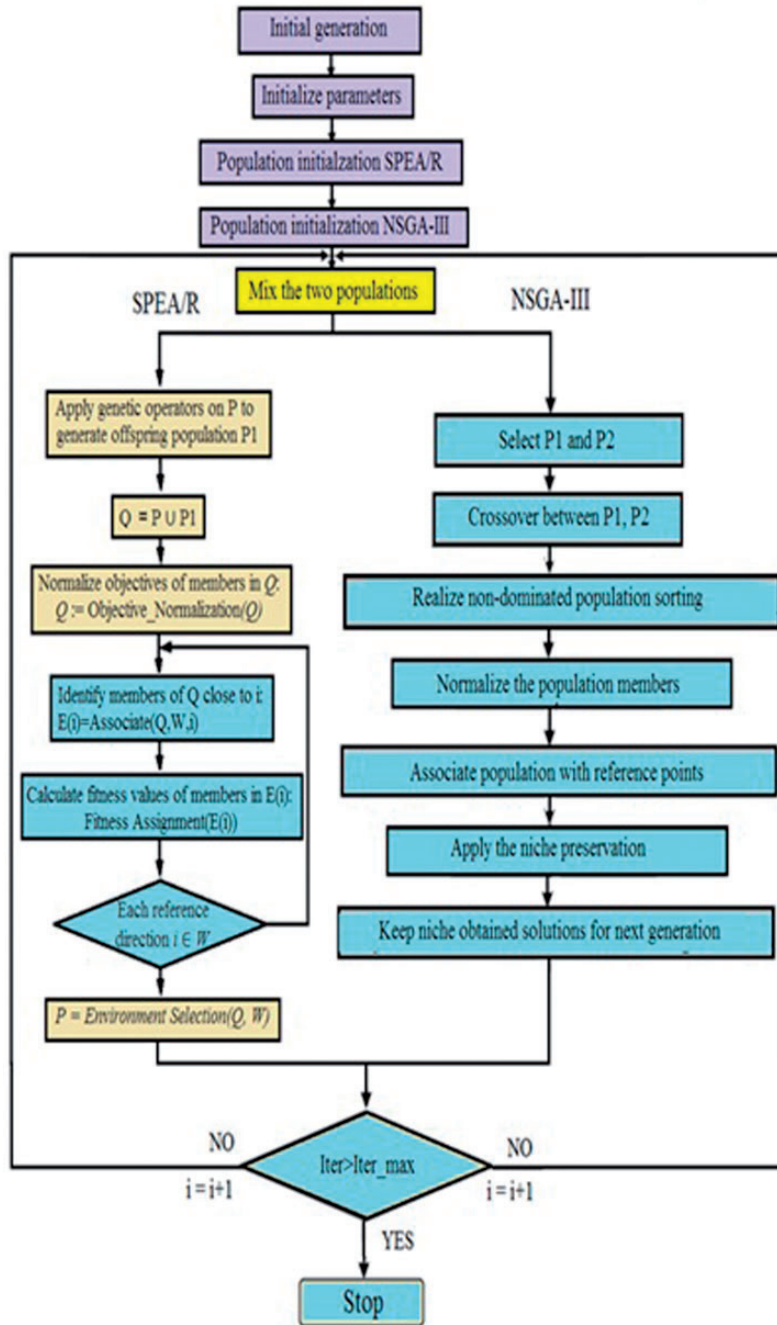
Figure 4. Flowchart of HNSGA-III&SPEA/R.

methods were run 20 times for test problems. The statistical results of 20 runs and parameters of the methods are shown in Tables 2 to 4.

The statistical results of the method for IGD are presented in Table 5. Hybrid methods (HNSGA-III&SPEA/ R) have been demonstrated on all statistics for two-goal test problems that are expressed through the IGD parameter. The performance of the accuracy and convergence of the method is reflected in the IGD index.

Therefore, it has been shown that the proposed HNSGA-III&SPEA/R method can provide outstanding convergence on the two target benchmarks. Pareto optimal solution of HNSGA-III&SPEA/R on each benchmark is also described in Figure 5 (UF8, UF10).

Table 1. Benchmark functions for test multi-objective optimization.

Mathematics formulation	Mathematics formulation	Mathematics formulation

UF2:

$$f_1 = x_1 + \frac{2}{|J_1|} \sum_{j \in J_1} y_j^2$$

$$f_2 = 1 - \sqrt{x} + \frac{2}{|J_2|} \sum_{j \in J_2} y_j^2$$

$$y_j = \begin{cases} \left[0.3x_1^2 \cos\left(24\pi x_1 + \frac{4j\pi}{n}\right) + 0.6x_1 \right] \sin\left(6\pi x_1 + \frac{j\pi}{n}\right) & \text{iff} j \in J_1 \\ \left[0.3x_1^2 \cos\left(24\pi x_1 + \frac{4j\pi}{n}\right) + 0.6x_1 \right] \sin\left(6\pi x_1 + \frac{j\pi}{n}\right) & \text{iff} j \in J_2 \end{cases}$$

$J_1 = \{j|j \text{ is odd and } 2 \leq j \leq n\};$
$J_2 = \{j|j \text{ is even and } 2 \leq j \leq n\};$

UF8:

$$f_1 = \cos(0.5x_1\pi)\cos(0.5x_2\pi) + \frac{2}{|J_1|} \sum_{j \in J_1} \left(x_j - 2x_2\sin\left(2\pi x_1 + \frac{j\pi}{n}\right) \right)^2$$

$$f_2 = \cos(0.5x_1\pi)\cos(0.5x_2\pi) + \frac{2}{|J_2|} \sum_{j \in J_2} \left(x_j - 2x_2\sin\left(2\pi x_1 + \frac{j\pi}{n}\right) \right)^2$$

$$f_3 = \sin(0.5x_1\pi) + \frac{2}{|J_3|} \sum_{j \in J_1} \left(x_j - 2x_2\sin\left(2\pi x_1 + \frac{j\pi}{n}\right) \right)^2$$

$J_1, J_2,$ and J_3 are the same as those of UF10.

UF4:

$$f_1 = x_1 + \frac{2}{|J_1|} \sum_{j \in J_1} h(y_j)$$

$$f_2 = 1 - x_2 + \frac{2}{|J_2|} \sum_{j \in J_2} h(y_j)$$

$$y_j = x_j - \sin\left(6\pi x_1 + \frac{j\pi}{n}\right)$$
$$j = 2, 3, \ldots, n$$
$$h(t) = \frac{|t|}{1 + e^{2|t|}}$$

J_1 and J_2 are the same as those of UF2.

UF10:

$$f_1 = \cos(0.5x_1\pi)\cos(0.5x_2\pi) + \frac{2}{|J_1|} \sum_{j \in J_1} (4y_j - \cos(8\pi y_j + 1))$$

$$f_2 = \cos(0.5x_1\pi)\cos(0.5x_2\pi) + \frac{2}{|J_1|} \sum_{j \in J_2} (4y_j - \cos(8\pi y_j + 1))$$

$$f_3 = \cos(0.5x_1\pi) + \frac{2}{|J_3|} \sum_{j \in J_3} (4y_j - \cos(8\pi y_j + 1))$$

UF5:

$$f_1 = x_1 + \left(\frac{1}{2N} + \varepsilon\right)|\sin(2N\pi x_1)| + \frac{2}{|J_1|} \sum_{j \in J_1} h(y_j)$$

$$f_2 = 1 - x_1 + \left(\frac{1}{2N} + \varepsilon\right)|\sin(2N\pi x_1)| + \frac{2}{|J_2|} \sum_{j \in J_2} h(y_j)$$

$$y_j = x_j - \sin\left(6\pi x_1 + \frac{j\pi}{n}\right)$$
$$j = 2, 3, \ldots, 4$$
$$h(t) = 2t^2 - \cos(4\pi t) + 1$$

J_1 and J_2 are the same as those of UF2, $\varepsilon > 0.$

$J_1 = \{j|3 \leq j \leq n \text{ and } j - 1 \text{ is a multiplication of 3}\}$
$J_2 = \{j|3 \leq j \leq n \text{ and } j - 2 \text{ is a multiplication of 3}\}$
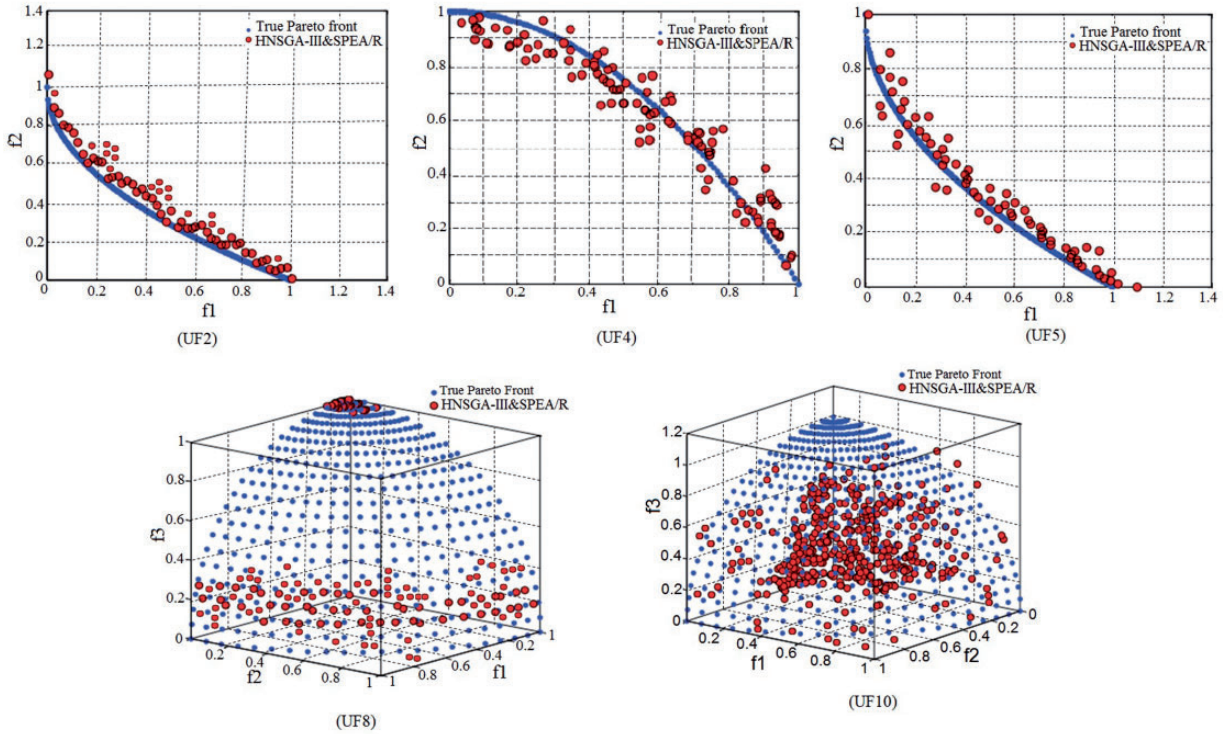$J_3 = \{j|3 \leq j \leq n \text{ and } j - 3 \text{ is a multiplication of 3}\}$

Figure 5. The resulting Pareto optimal solution of HNSGA-III&SPEA/R on each benchmark functions.

Table 2. NSGA-III algorithm parameters.

Maximum number of iterations	MaxIt = 10000	Number of parnets (offsprings)	nCrossover = 2*round (pCrossover*nPop/2)
Population size	nPop = 100	Number of mutants	nMutation = round (pMutation*nPop)
Crossover percentage	pCrossover = 0.5	Mutation step size	sigma = 0.1*(VarMax − VarMin)
Mutation percentage	pMutation = 0.5	Generating reference points	nDivision = 10 Zr = Generate ReferencePoints(nObj, nDivision);
Mutation rate = 0.02	mu = 0.02	Number of parnets (offsprings)	nCrossover = 2*round(pCrossover*nPop/2)

Table 3. SPEA/R algorithm parameters.

Maximum number of iterations	10,000	pMutation	1 − pCrossover
Population size	100	nMutation	nPop − nCrossover
Archive size	50	mutation_params.h	0.2
KNN parameter	Round(sqrt(nPop + nArchive))	crossover_params.gamma	0.1
pCrossover	0.7	crossover_params.VarMin	VarMin
nCrossover	Round(pCrossover*nPop/2)*2	mutation_params.VarMin	VarMin
mutation_params.VarMax	VarMax	crossover_params.VarMax	VarMax

The Pareto front result is shown in Figure 5. Numerical results have shown that the HNSGA-III&SPEA/R method has higher accuracy for benchmarking functions with two objectives related to convergence and coverage. However, for some tri-objective functions, the three targets are standard; although the proposed method shows high convergence, it has low coverage. Therefore, we can confirm that the HNSGA-III&SPEA/R method has advantages over the NSGA-III and SPEA/R methods, which are the higher convergence and coverage characteristics. In addition, in most cases, the results of HNSGA-III&SPEA/R are better than that of NSGA-III and

Table 4. HNSGA-III&SPEA/R algorithm parameters.

Maximum number of iterations	10,000	pMutation	1-pCrossover
Population size	100	nMutation	nPop-nCrossover
Archive size	50	mutation_params.h	0.2
KNN parameter	Round(sqrt(nPop + nArchive))	crossover_params.gamma	0.1
pCrossover	0.7	crossover_params.VarMin	VarMin
nCrossover	Round(pCrossover*nPop/2)*2	mutation_params.VarMin	VarMin
mutation_params.VarMax	VarMax	crossover_params.VarMax	VarMax
Mutation rate	0.02	Mutation step size	0.1*(VarMax − VarMin)
Number of parnets (offsprings)	2*round(pCrossover*nPop/2)	Mutation step size	0.1*(VarMax − VarMin)
Number of mutants	Round(pMutation*nPop)		

Table 5. Results for IGD.

IGD	Average	Median	STD Dev	Worst	Best
IGD					
SPEA/R	0.07144	0.04523	0.03744	0.14521	0.03636
NSGA-III	0.12244	0.1242	0.01243	0.14485	0.10454
HNSGA-III&SPEA/R	0.01351	0.01544	0.00245	0.01456	0.01274
UF4					
SPEA/R	0.13433	0.14445	0.00643	0.15454	0.12344
NSGA-III	0.06823	0.06835	0.00254	0.07078	0.06424
HNSGA-III&SPEA/R	0.02645	0.02867	0.00145	0.02734	0.02267
UF5					
SPEA/R	2.50643	2.42522	0.57098	3.03544	1.48643
NSGA-III	1.26755	1.33741	0.13839	1.46735	0.12145
HNSGA-III&SPEA/R	0.47843	0.45450	0.08445	0.53561	0.22371
UF8					
SPEA/R	0.23639	0.43870	0.13765	0.45467	0.24565
NSGA-III	0.56681	0.53667	0.28667	0.69647	0.28530
HNSGA-III&SPEA/R	0.19639	0.27870	0.06765	0.33467	0.17565
UF10					
SPEA/R	1.70324	1.54303	0.55103	3.03811	1.13805
NSGA-III	1.63529	1.59123	0.29349	2.16232	1.22048
HNSGA-III&SPEA/R	1.70344	1.54333	0.55135	3.03833	1.13821

SPEA/R. Therefore, the HNSGA-III&SPEA/R method has better results and more accurate than the other two methods because it uses simple operators to create a new population derived from a non-dominant solution.

In addition, density estimation tool based on effective reference direction has been used in SPEA/R algorithm, new physical assignment diagram, and new environment selection. The individuals of HNSGA-III&SPEA/R are updated for each generation, thus supporting search agents to explore the search space more widely.

Vibration characteristic of the powertrain mount system

Mathematical model

Full car model with 10 degrees of freedom is shown in Figure 1. Suspension and tires are considered spring and damping systems. Where the masses $m_{2.1}$, $m_{2.2}$, $m_{2.3,}$ and $m_{2.4}$ denote the weight of four wheels (the mass does not burst). The masses m_{cg1} and m_{cab} represent the mass (unburnt mass) of the frame and engine, respectively. $Z3.1$, $Z3.2$, $Z3.3$, and $Z3.4$ are the vertical displacements of the wheel, and $Z1$ and $Z2$ are, respectively, the vertical displacement of the frame and the transmission system. And (Roll and Altitude) are vibrations that rotate around the corresponding X and Y axes. Next, the symbols Φ and Ψ represent the pitch and roll of the frame. The inertia of the transmission system on the y-axis and the x-axis is Iyy and Ixx, respectively, and the inertial moment for the chassis on axes $X1$ and $Y1$ is $Iyy1$ and $Ixx1$, respectively. The stiffness and damping parameters of the wheels are

Table 6. Parameters of the mathematical model.

Symbol	Parameters of the mathematical model
X_i	Vector-column of displacements and angular oscillations of masses.
M	The matrix of inertial coefficients of car parts.
C	The matrix of coefficients of stiffnesses and torsional rigidity.
K	The matrix of damping coefficients.
Q(t)	Column vector of the perturbing forces and moments.
	$q_2(t) = q_1(t + \tau)$ with τ: time interval, *va*: vehicle speed.

K3.1, *K3.2*, *K3.3*, and *K3.4* and *C3.1*, *C3.2*, *C3.3*, and *C3.4*, respectively. Similarly, the hardness and damping parameters of primary suspension are K2.1, K2.2, K2.3, and K2.4 and C2.1, C2.2, C2.3, and C2.4, respectively, while the hardness and damping parameters of the drive system are *K1.1*, *K1.2*, and *K1.3* and *C1.1*, *C1.2*, and *C1.3*, respectively. The distance of the front and rear support from the center (*CG*) of the transmission system is *a* and *b*, respectively, and the right and left mounting distances from the *CG* of the transmission system are *c* and *d*, respectively. *a1*, *b1*, and *c1*, *d1*.

By using Newton's law, the mathematical model of Figure 1 can be written as given below

$$\mathbf{M}\ddot{\mathbf{x}}_i + \mathbf{K}\dot{\mathbf{x}}_i + \mathbf{C}\mathbf{x}_i = \mathbf{Q}(t) \tag{2}$$

where the symbols are shown in Table 6.

The multi-object optimization function of the engine mount system

There are many indicators to evaluate the vibration of the powertrain. In particular, mean square acceleration oscillates at the front and rear, right and left of the engine mount system, the mean square displacement difference between the engine and vehicle chassis at the front and rear, and right and left engine mount system. These are two important parameters that determine the decisive influence of powertrain vibration on chassis. In order to optimally reduce the vibration of the powertrain, we need to simultaneously optimize the parameters of mean square acceleration and mean square displacement at the front and rear, right and left of the engine mounts.

The average square value of the vibration acceleration of any points can be determined by the formulas

$$\ddot{z}_c = \sqrt{\int_{-\infty}^{\infty} S\ddot{z}(\omega)d\omega} = \sqrt{\int_{-\infty}^{\infty} \omega^4 |W_z(j\omega)|^2 \, S_q(\omega)} \tag{3}$$

where ω: frequency;

$W_z(j\omega)$: squared modulus of amplitude and phase characteristics;

$S_q(\omega)$: spectral density of exposure.

The modules of the amplitude and phase characteristics of the vibratory displacement of the powertrain and the car body in the place of the front mount are

$$W^{O_1}(j\omega) = W_0(j\omega) + W_0^{\varphi}(j\omega) \cdot l_3 \tag{4}$$

$$W_{ca}^{O_1}(j\omega) = W_{ca}^{\varphi}(j\omega) + W_{ca}(j\omega) \cdot l_6 \tag{5}$$

where

$W_0(j\omega)$: module amplitude-phase characteristics in the center of the car body;

$W_0^{\varphi}(j\omega)$: module amplitude-phase characteristics of the longitudinal-angular body of the car;

$W_k^{O_1}(j\omega)$: module of the amplitude and phase characteristics of the body in place of the front mount of the powertrain;

$W_{ca}(j\omega)$: module amplitude-phase characteristics in the center of the powertrain of the car;

$W_{ca}^{\varphi}(j\omega)$: module amplitude-phase characteristics of the longitudinal-angular powertrain of the car;

$W_{ca}^{O_1}(j\omega)$: modulus of amplitude and phase characteristics in place of the front mount of the powertrain.
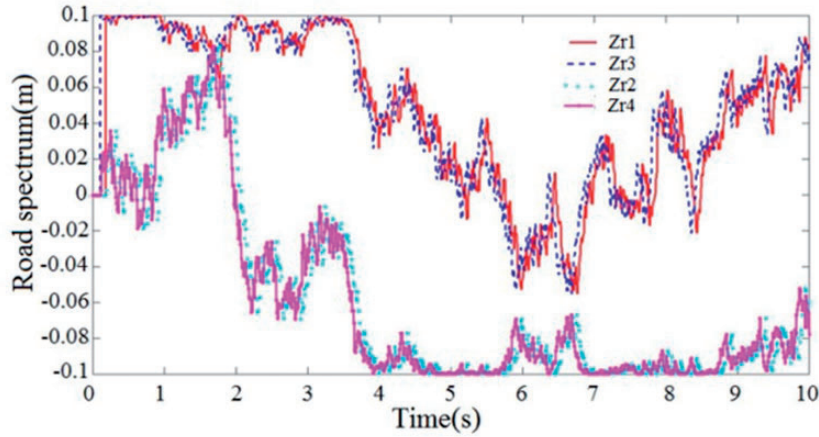
Figure 6. Road surface profiles. Zr1 and Zr3 correspond to the right front and rear wheel. Zr2 and Zr4 correspond to the left front and rear wheel.

The modules of the amplitude and phase characteristics of the vibration displacement of the powertrain and the car body in the place of the rear mount are

$$W^{O_2}(j\omega) = W_0(j\omega) + W_0^{\varphi}(j\omega) \cdot l_4 \tag{6}$$

$$W_{ca}^{O_2}(j\omega) = W_{ca}(j\omega) - W_{ca}^{\varphi}(j\omega) \cdot l_7 \tag{7}$$

where

$W_k^{O2}(j\omega)$: the module of the amplitude-phase characteristics of the body in the place of the rear mount of the powertrain;

$W_{ca}^{O2}(j\omega)$: the module of amplitude and phase characteristics in the place of the rear mount of the powertrain.

The difference of the module frequency response of the vibration of the powertrain and the car body in place of the front mount of the powertrain

$$W_{ca-}^{O_1}(j\omega) = W_{ca}^{O_1}(j\omega) - W^{O_1}(j\omega) \tag{8}$$

The difference of the frequency response module of the vibration displacement of the powertrain and the car body at the rear mount

$$W_{ca-}^{O_2}(j\omega) = W_{ca}^{O_2}(j\omega) - W^{O_2}(j\omega) \tag{9}$$

Simulated input parameters

Road surface profiles. When the vehicle moves, there are many factors that cause the vibration. The factors are: the internal force in the car; external forces appear in the process of using acceleration, braking, revolving; exterior conditions such as wind and storm; boring face street. Among the factors on the bumpy side of the road is the oscillation cause of the vehicle. To simulate the most general calculation, we use the road surface profile as a random function as shown in Figure 6, and simulated parameters are shown in Table 7.

Simulation results of application HNSGA-III&SPEA/R method to optimization of the powertrain mount system stiffness parameter

Through Matlab, we calculated six functions of acceleration and displacement according to the stiffnesses of the front left, front right, and rear engine mount (K1.1, K1.2, and K1.3) value as shown in Figure 7 (Figures 7 and 8 show the results in the form of 4D space via the isosurface function in Matlab).

Table 7. Model parameters.

No.	Parameter	Value	unit
1	$M_{2.1}, m_{2.2}, m_{2.3}, m_{2.4}$	60	kg
2	m_{cab}, m_{cg1}	1000, 1200	kg
3	$K2.1, K2.2, K2.3, K2.4$	37,000	N/m
4	$C2.1, C2.2, C2.3, C2.4$	700	N-s/m
5	$K3.1, K3.2, K3.3, K3.4$	55,000	N/m
6	$C3.1, C3.2, C3.3, C3.4$	4000	N-s/m
7	$K1.1, K1.2, K1.3$	670,000	N/m
8	$C1.1, C1.2, C1.3$	6000	N-s/m
9	a, b, c = d	0.187, 0.623, 0.3	m
10	a1 = b1, c1 = d1	1.5,1	m
11	Ixx, Iyy	320, 80	Kg m^2
12	Ixx1, Iyy1	4000, 950	Kg m^2
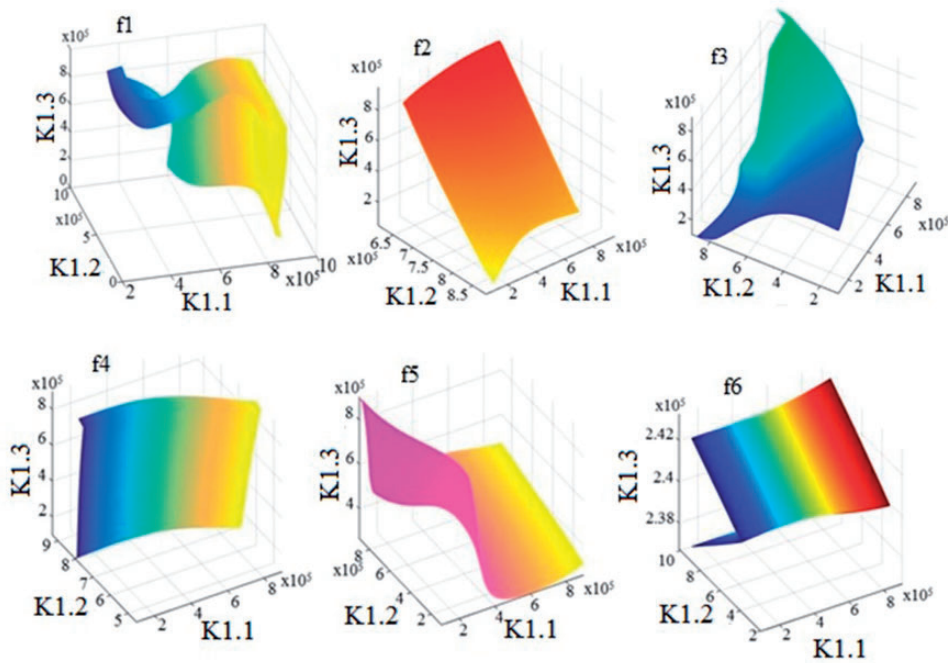
Figure 7. Values of six-objective optimization functions.

Values of six-objective functions according to the stiffnesses (K1.1, K1.2, and K1.3). f1 is mean square displacement (MSD) at the front left engine mount, f2 is mean square acceleration (MSA) at the front left engine mount, f3 is MSD at the front right engine mount, f4 is MSA at the front right engine mount, f5 is MSD at the rear engine mount, and f6 is MSA at the rear engine mount.

It is well known that the results of multi-objective optimization would be a set of non-dominated optimized points, called Pareto set. These points offer a wide range of parameters to the designer to choose the optimum point depending on his designing conditions. There are always conflicting objective functions in vehicle designing which improvement in one function may have an unfavorable influence on other functions. In this article, multi-objective optimization for all six-objective functions is done simultaneously. While applying the HNSGA-III&SPEA/R optimization algorithm, we obtain results as shown in Figure 8.

The average square of the Pareto front of MSD at the front left engine mount: f1 = 4.1318e-05 (m).

The average square of the Pareto front of MSA at the front left engine mount: f2 = 1.4942 (m/s^2).

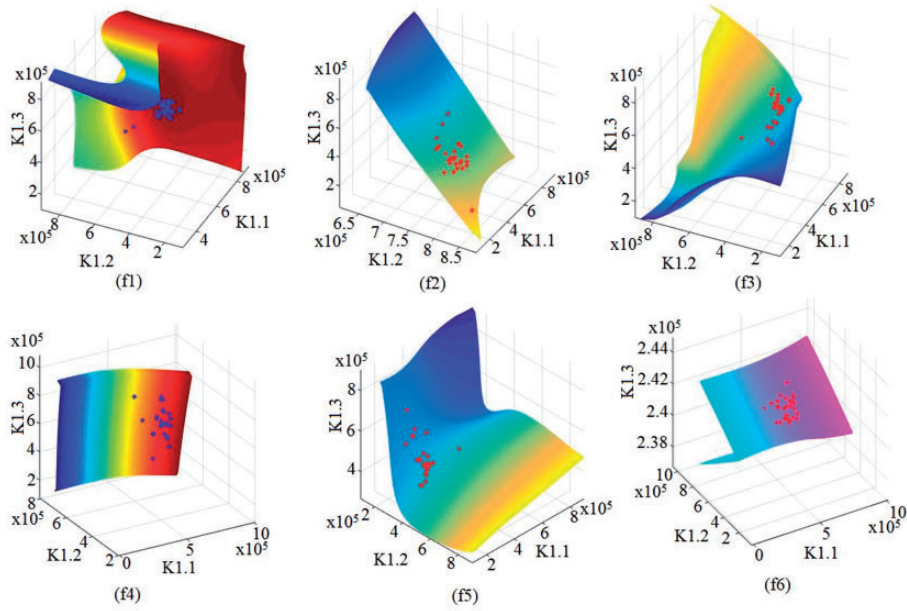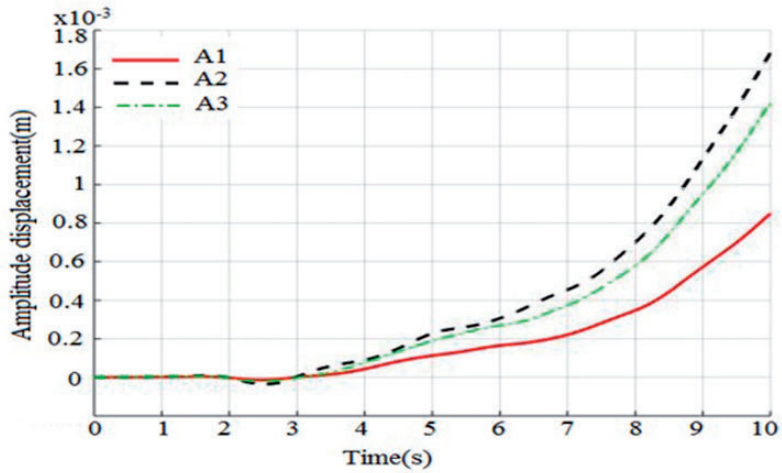**Figure 8.** Pareto front set of six-optimization objective.
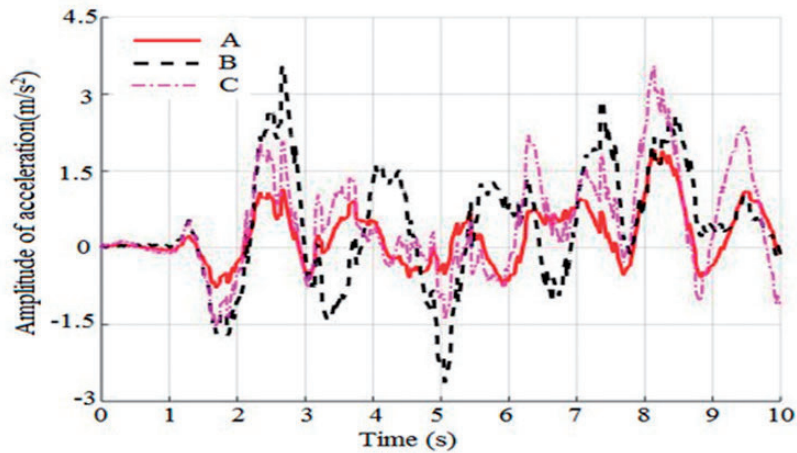

Figure 9. Acceleration of the vehicle frame.

Figure 10. Displacement of the vehicle frame.

The average square of the Pareto front of MSD at the front right engine mount: f3 = 5.2547e-05 (m).
The average square of the Pareto front of MSA at the front right engine mount: f4 = 1.7114 (m/s^2).
The average square of the Pareto front of MSD at the front right engine mount: f5 = 2.3641e-05 (m).
The average square of the Pareto front of MSA at the front right engine mount: f6 = 1.4004 (m/s^2).

where f1: Pareto front of MSD at the front left engine mount; f2: Pareto front of MSA at the front left engine mount. f3: Pareto front of MSD at the front right engine mount; f4: Pareto front of MSA at the front right engine mount; f5: Pareto front of MSD at the rear engine mount; f6: Pareto front of MSA at the rear engine mount.

Application of HNSGA-III&SPEA/R optimization algorithm with six-objective functions (f1, f2, f3, f4, f5, and f6): the red dots on f2, f3, f5, and f6 and the blue dots on f1 and f4 are the result set of the Pareto front that the HNSGA-III&SPEA/R algorithm has found.

Conclusion

A new hybrid optimization method has been proposed to address the multi-objective optimization issues. Optimization through the random search method is at the heart of this new hybrid method. The new hybrid method based on Pareto Strength evolution algorithm (SPEA/R) and NSGA-III genetic algorithm developed to find global optimization. The efficient HNSGA-III&SPEA/R hybrid method is evaluated through the use of a variety of benchmarking functions for two objectives and three goals. The results are compared with other multi-purpose optimization methods such as SPEA/R and NSGA-III. The numerical results have shown that the proposed hybrid method has a higher efficiency in solving multi-objective optimization problems with much better convergence and coverage. HNSGA-III&SPEA/R has been applied in the problem of Powertrain mount system stiffness parameters optimization. Simulation results comparing one of the results in the set of the Pareto front from the HNSGA-III&SPEA/R algorithm with different stiffness values (K1.1, K1.2, and K1.3) are shown in Figures 9 and 10.

Figure 9 shows the acceleration of the vehicle frame corresponding to the different stiffness values. Symbol A corresponds to the optimal stiffness value in a set of the Pareto front. Symbol B corresponds to K1.1 = 270,000; K1.2 = 380,000; K1.3 = 550,000. Symbol C corresponds to K1.1 = 780,000; K1.2 = 750,000; K1.3 = 340,000. From the graph, we see that the smallest acceleration is at the optimal stiffness value. Similarly, Figure 10 shows the displacement of the vehicle frame corresponding to the different stiffness values. Symbol A1 corresponds to the optimal stiffness value in a set of the Pareto front. Symbol A2 corresponds to K1.1 = 280,000; K1.2 = 350,000; K1.3 = 750,000. Symbol A3 corresponds to K1.1 = 780,000; K1.2 = 740,000; K1.3 = 660,000. From the graph, we see that the smallest displacement is at the optimal stiffness value in a set of the Pareto front.

Thus, this paper has presented a new hybrid algorithm to calculate the optimal parameters simultaneously. This algorithm gives relatively accurate results, and this has been evaluated through the standard functions. Next, this algorithm is used to calculate six optimal stiffness parameters simultaneously for the engine mount system. The results of the algorithm have found out the optimal parameters of the engine mount, which makes the mount system eliminate unwanted vibrations to the chassis better than the previous methods.

ORCID iD

Dinh-Nam Dao ⓘD https://orcid.org/0000-0001-9810-2096

References

1. Yu YH and Naganathan NG, RV. A literature review of automotive vehicle engine mounting systems. *Mech Mach Theory* 2001; 36: 123–142.
2. Adiguna H, Tiwari M, Singh R, et al. Transient response of a hydraulic engine mount. *J Sound Vib* 2003; 268: 217–248.

3. Konak A, Coit D and Smith E. Multi-objective optimization using genetic algorithms. *Reliab Eng Syst Safety* 2006; 91: 92–107.

4. Deb K, Pratap A, Agarwal S, et al. A fast elitist multiobjective genetic algorithm: NSGA-II. *IEEE Trans Evol Computat* 2002; 6: 182–197.

5. Chang LC and Chang FJ. Multi-objective evolutionary algorithm for operating parallel reservoir system. *J Hydrol* 2009; 377: 12–20.

6. Ishibuchi H, Tsukamoto N. and Nojima Y, Evolutionary many-objective optimization: a short review. In: *Proceedings of IEEE congress on evolutionary computation*, Hong Kong, June 2008, pp.1–6.

7. Malekmohammadi B, Zahraie B and Kerachian R. A ranking solution of multi-objective reservoir operation optimization models using multi-criteria decision analysis. *Expert Syst Appl* 2011; 38: 7851–7863.

8. Kalyanmoy D. *Handling many-objective problems using an improved NSGA-II procedure*. In: *CEC 2012: proceedings of IEEE congress on evolutionary computation*, Brisbane, Australia, 10–15 June 2012.

9. Deb K and Jain H. An evolutionary many objective optimization algorithms using reference-point based non-dominated sorting approach, part I: solving problems with box constraints evolutionary computation. *IEEE Trans Evol Computat* 2014; 18: 577–601.

10. Kim M, Hiroyasu T, Miki M, et al. SPEA2+: improving the performance of the Strength Pareto evolutionary algorithm 2. In: Yao X, et al. (eds) *PSN 2004: parallel problem solving from nature – PPSN VIII*, 2004. Berlin, Heidelberg: Springer. *Lecture notes in computer science*, vol. 3242, 777–784.

11. Zitzler E, Laumanns M and Thiele L. Evolutionary methods for design optimization and control with applications to industrial problems in Athens, Greece. *Int Center Num Method Eng* 2001; 18(3): 95–100.

12. Borisevic J and Bartlett LM. Safety system optimization by improved strength Pareto evolutionary approach (SPEA2) in UK 2007. In: *Proceedings of the 17th advances in reliability technology symposium (ARTS)*, Loughborough, UK, 2007, pp.38–49. https://repository.lboro.ac.uk/articles/online_resource/Safety_system_optimization_by_improved_strength_Pareto_evolutionary_approach_SPEA2_/9223406/1

13. Hiroyuki M and Hiroki K. Modified SPEA2 for probabilistic reliability assessment in smart grids, complex adaptive systems. *Proc Comput Sci* 2011; 6: 1435–1440.

14. De Tommasi L, Beelen TGJ, Sevat MF, et al. *Multi-objective optimization of RF circuit blocks via surrogate models and NBI and SPEA2 methods*. CASA Report Eindhoven 2011. Eindhoven: Technische Universiteit Eindhoven, 2011, Vol. 1132.

15. Sokratis S and George T. Studying the SPEA2 algorithm for optimising a pattern-recognition based machine translation system. In: *Proceedings of the 2011 IEEE symposium on computational intelligence in multicriteria decision-making (MCDM 2011)*, Paris, France, 11–15 April 2011, pp.97–104. Piscataway, NJ: IEEE. DOI: 10.1109/SMDCM.2011.5949279.

16. Zhao F, Lei W, Ma W, et al. An improved SPEA2 algorithm with adaptive selection of evolutionary operators scheme for multiobjective optimization problems. *Math Probl Eng* 2016; 8: 20.

17. Hamida IB, Salah SB, Msahli F, et al. Strength Pareto evolutionary algorithm 2 for environmental/economic power dispatch. In: *ICMIC 2015: 7th international conference on modelling, identification and control*, Tunisia, 18–20 December 2015.

18. Jiang S and Yang S. A strength Pareto evolutionary algorithm based on reference direction for multiobjective and many-objective optimization. *IEEE Trans Evol Computat* 2017; 21(3): 329–346.

19. Mirjalili S, Saremi S, Mirjalili SM, et al. Multi-objective grey wolf optimizer: a novel algorithm for multi-criterion optimization. *Expert Syst Appl* 2016; 47: 106–119.

20. Premalatha K, Natarajan AM, Hybrid PSO, et al. Maximization. *Int J Open Probl Comp* 2009; 2: 597–608.

21. Velazquez OJ, Coello CC and Arias-Montano A. Multi-objective compact differential evolution. In: *IEEE symposium on differential evolution*, 2014, pp.1–8. Piscataway, NJ: IEEE. DOI: 10.1109/SDE.2014.7031534.

22. Hemmatian H, Fereidoon A and Assareh E. Optimization of hybrid laminated composites using the multi-objective gravitational search algorithm (MOGSA). *Eng Optim* 2014; 46: 1169–1182.

23. Shi X and Kong D. A multi-objective ant colony optimization algorithm based on elitist selection strategy. *Metall Mining Indus* 2015; 7: 333–338.

24. Hancer E, Xue B, Zhang M, et al. A multi-objective artificial bee colony approach to feature selection using fuzzy mutual information. In: *IEEE congress on evolutionary computation (CEC)*, 2015, pp.420–2427. DOI: https://doi.org/10.26686/wgtn.14220071.v1.

25. Lin W, Yu DY, Zhang C, et al. A multi-objective teaching-learning-based optimization algorithm to scheduling in turning processes for minimizing makespan and carbon footprint. *J Clean Prod* 2015; 101: 337–347.

26. Jeong S, Hasegawa S, Shimoyama K, et al. Investigation of efficient GA/PSO-hybrid algorithm applicable to real-world design optimization. In: *2009 IEEE congress on evolutionary computation*, 2009, pp. 777–784. Piscataway, NJ: IEEE. DOI: https://doi.org/10.1109/CEC.2009.4983024.

27. Bai H-B. An improved multi-objective particle swarm optimization. *IJCO* 2016; 3: 105–120.

28. Zandavi P. A hybrid simplex non-dominated sorting genetic algorithm for multiobjective optimization. *Int J Swarm Intel Evol Comput* 2016; 5(3).

29. Yang G, Xu T, Li X, et al. An efficient hybrid algorithm for multiobjective optimization problems with upper and lower bounds in engineering. *Math Probl Eng*. 2015; 2015: 13. DOI: 10.1155/2015/932029.
30. Rashidi E, Jahandar M and Zandieh M. An improved hybrid multi-objective parallel genetic algorithm for hybrid flow shop scheduling with unrelated parallel machines. *Int J Adv Manuf Technol* 2010; 49: 1129–1139.
31. Zhang Q, Zhou A and Zhao S. Multi-objective optimization test instances for the CEC 2009 special session and competition. Colchester, UK: University of Essex, Colchester, UK and Nanyang Technological University, 2008, pp.1–30.